LIGHTCURVE INVERSION FOR 65 CYBELE

Lorenzo Franco
Balzaretto Observatory (A81), Rome, ITALY
lor_franco@libero.it

Frederick Pilcher
Organ Mesa Observatory
4438 Organ Mesa Loop
Las Cruces, NM 88011 USA

(Received: 2015 April 11)

We present a shape and spin axis model for main-belt asteroid 65 Cybele. The model was obtained with lightcurve inversion process, using combined dense photometric data obtained during fifteen apparitions from 1977 to 2014 and sparse data from USNO Flagstaff. Analysis of the resulting data found a sidereal period P = 6.081434 ± 0.000005 hours and two possible pole solutions: (λ = 208°, β = –7°) and (λ = 27°, β = –14°) with an error of ±15 degrees.

The main-belt asteroid 65 Cybele has been observed for fifteen apparitions from 1977 to 2014 with a variety of phase angles and phase angle bisectors. Dense photometric data were downloaded from the Asteroid Photometric Catalogue (APC) by Lagerkvist *et al.* (2001) and from the Asteroid Light Curve Database (ALCDEF, 2014). The observational circumstances for the fifteen apparitions are reported in Table I.

Year	#LCs	Data Points	PA°	PABL°	PABB°	Ref.
1977	3	150	2/3	332	0	(1)
1978	1	9	-3	38	-4	(1)
1982	11	92	17/16	213/219	3/4	(2)
1983	11	119	18	299/314	3/1	(2)
1984	2	29	17/12	10/16	2/3	(2)
1985/6	3	91	11/12	73	-4	(2)
1987	1	44	4	126	-2	(3)
1988	1	63	3	189	2	(3)
1989	1	28	4	272	4	(4)
1994	2	44	7/5	165	0	(5)
2007	2	56	5	182	2	(6)
2009	7	1590	12/2	345	-1	(7)
2010/1	5	1234	12/15	46/49	-4	(6) (8)
2011/2	6	1841	11/1	99	-4	(9)
2014	5	1030	2/8	264	4	(10)

Table I. Observational circumstances for 65 Cybele over fifteen apparitions. A total of 61 lightcurves were used for lightcurve inversion analysis. PA, PABL and PABB are, respectively, the phase angle, phase angle bisector longitude and latitude. References: (1) Schober *et al.* (1980); (2) Weidenschilling *et al.* (1987); (3) Weidenschilling *et al.* (1990); (4) Gil Hutton (1990); (5) Shevchenko *et al.* (1996); (6) Behrend web; (7) Pilcher and Stephens (2010); (8) Pilcher (2011); (9) Pilcher (2012); (10) Pilcher (2014)

In order to improve the solution, we also used sparse data from USNO Flagstaff Station, as has been shown by Kaasalainen (2004) and Ďurech *et al.* (2009). Sparse data were taken from the Asteroids Dynamic Site (AstDyS-2, 2014) for a total of 484 data points (Figure 2). Figure 1 (left) shows the phase angle bisector (PAB) longitude distribution for dense and sparse data points from 689 USNO Flagstaff station. Figure 1 (right) shows the PAB latitude distribution.

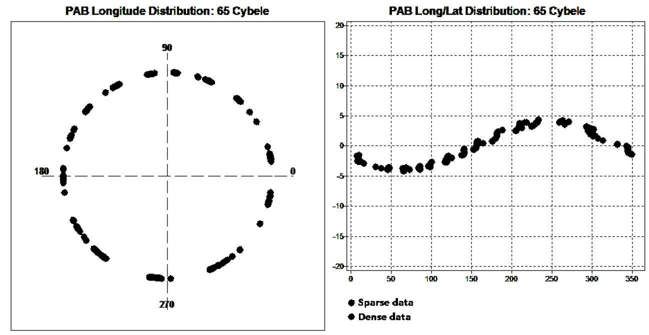

Figure 1. PAB longitude and latitude distribution of the data used for lightcurve inversion model. Dense data are in blue and sparse data are in red.

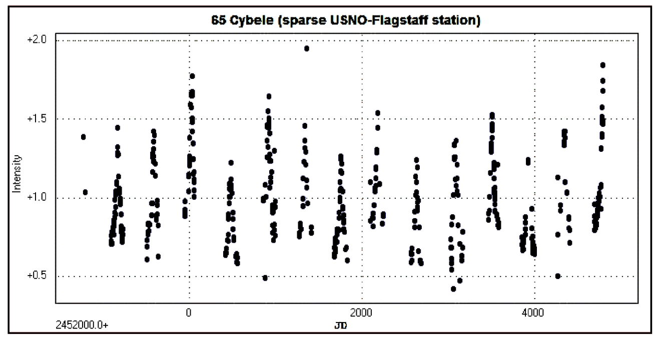

Figure 2. Sparse photometry data points from 689 USNO Flagstaff station.

Lightcurve inversion was performed using *MPO LCInvert* v.11.1.0.2 (Bdw Publishing), which implements algorithms and code provided by Mikko Kaasalainen and Josef Ďurech. For guidelines and a description of the modeling process see the *MPO LCInvert* operating instructions manual and Warner *et al.* (2008).

All data from the sixty-one dense lightcurves and one sparse dataset were imported in *MPO LCInvert* for analysis, assigning them a different weighting factor, from 1.0 for the dense data to 0.3 for sparse data. The period search was started around the average of the synodic periods previously published in the literature. The search process found an isolated sidereal period with lowest chi-square value (Figure 3).

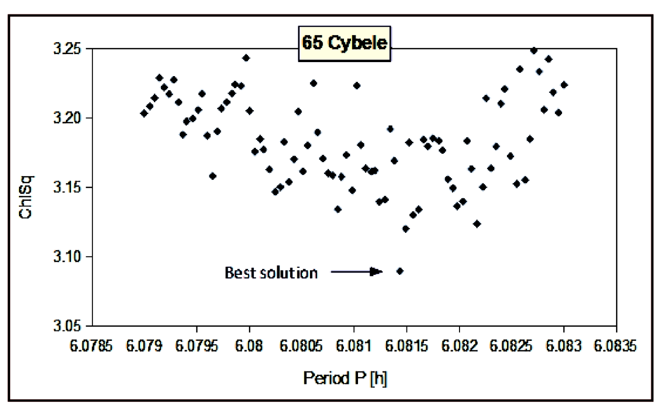

Figure 3. The period search for 65 Cybele shows an isolated minimum.

The pole search was started using the "medium" search option (312 fixed pole positions with 15° longitude-latitude steps) and the previously found sidereal period allowed to "float." The "dark facet" weighting factor was set to 1.8 to keep the dark facet area below 1% of total area and the number of iterations of processing was set to 75.

Data analysis shows the two lower chi-square solutions with a possible ambiguity for $\lambda \pm 180°$ at ($\lambda = 208°$, $\beta = -7°$) and ($\lambda = 27°$, $\beta = -14°$) with a sidereal period $P = 6.081434 \pm 0.000005$ h; see Figure 4 for log(chi-square) values distribution.

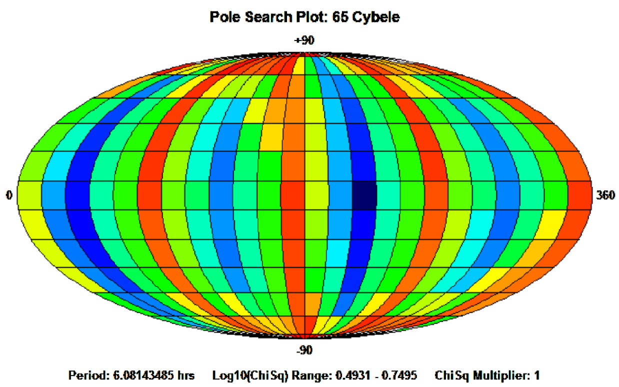

Figure 4. The pole search plot. Darker blue indicates the better solutions while red indicates the least-favorable solutions.

Typical errors in the pole solution are ±15 degrees and the uncertainty in period has been evaluated as a rotational error of 15° over the total time-span of the dense observations. This pole solution agrees with those reported by Pilcher (2011) using the simple amplitude-aspect method and found by Durech (private communication) using lightcurve inversion method with a similar dataset.

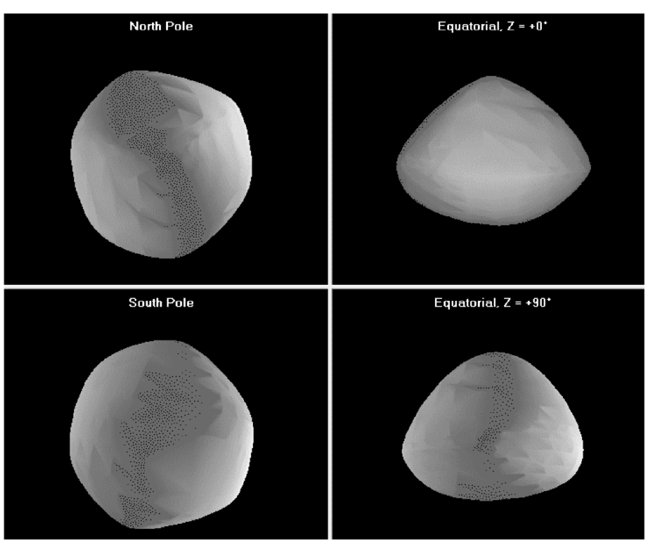

Figure 5. The shape model for 65 Cybele ($\lambda = 208°$, $\beta = -7°$).

Figure 5 shows the shape model (first solution) while Figure 6 shows the fit between the model (black line) and observed lightcurves (red points).

The model and the data will be stored in Database of Asteroid Models from Inversion Techniques (DAMIT; Ďurech 2015).

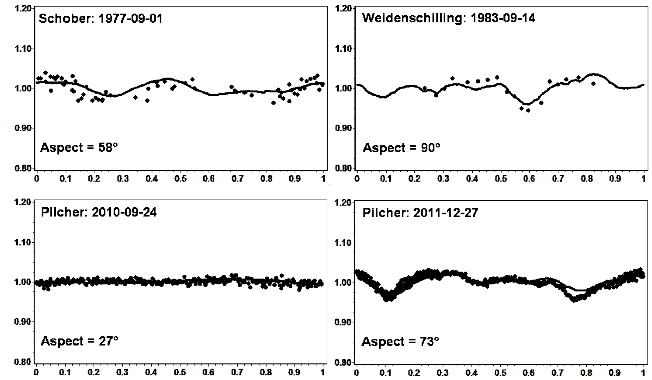

Figure 6. Model fit (black line) versus observed lightcurves (red points)

Acknowledgement

The authors thank Dr. Josef Durech for his advice.

References

ALCDEF (2013). *http://www.minorplanetcenter.net/light_curve2/light_curve.php*

AstDyS-2 (2014). Asteroids - Dynamic Site. *http://hamilton.dm.unipi.it/astdys/index.php?pc=0*

Bdw Publishing (2012). *http://www.minorplanetobserver.com/MPOSoftware/MPOLCInvert.ht*m

Behrend, R. Observatoire de Genève web site. *http://obswww.unige.ch/~behrend/page3cou.html*

DAMIT (2015). Database of Asteroid Models from Inversion Techniques. *http://astro.troja.mff.cuni.cz/projects/asteroids3D/web.php*

Ďurech, J., Kaasalainen, M., Warner, B.D., Fauerbach, M., Marks, S.A., Fauvaud, S., Fauvaud, M., Vugnon, J.-M., Pilcher, F., Bernasconi, L., Behrend, R. (2009). "Asteroid models from combined sparse and dense photometric data." *Astronomy and Astrophysics* **493**, 291-297.

Hutton, R.G. (1990). "V+B Photoelectric Photometry of Asteroids 65 Cybele and 216 Kleopatra." *Minor Planet Bul.* **17**, 34-35

Kaasalainen, M. (2004). "Physical models of large number of asteroids from calibrated photometry sparse in time." *Astronomy and Astrophys.* **422**, L39-42.

Lagerkvist C.-I., Piironen J., Erikson A., eds. (2001). *Asteroid Photometric Catalogue, 5th edition*. Astronomical Observatory, Uppsala University, Sweden. 201 pp.

Pilcher, F., Stephens, R.D. (2010). "Rotation Period Determination for 65 Cybele." *Minor Planet Bul*. **37**, 8.

Pilcher, F. (2011). "Rotation Period Determinations for 27 Euterpe, 296 Phaetusa and 672 Astarte, and a Note on 65 Cybele." *Minor Planet Bul*. **38**, 50-52.

Pilcher, F. (2012). "Rotation Period Determinations for 31 Euphrosyne, 65 Cybele, 154 Bertha 177 Irma, 200 Dynamene, 724 Hapag, 880 Herba, and 1470 Carla." *Minor Planet Bul*. **39**, 57-60.

Pilcher, F. (2014). "Rotation Period Determinations for 24 Themis, 65 Cybele 108 Hecuba, 530 Turandot, and 749 Malzovia." *Minor Planet Bul*. **41**, 250-252.

Schober, H.J., Scaltriti, F., Zappala, V., Harris, A.W. (1980) "The remaining large minor planets with unknown rotational properties - 31 Euphrosyne and 65 Cybele." *Astronomy and Astrophysics* **91**, 1-6.

Shevchenko, V.G., Chiorny, V.G., Kalashnikov, A.V., Krugly, Yu.N., Mohamed, R.A., Velichko, F.P. (1996). "Magnitude-phase dependences for three asteroids." *Astronomy and Astrophysics Supplement* **115**, 475-479.

Warner, B.D., Ďurech, J., Faurerbach, M., Marks, S. (2008). "Shape and Spin Axis Models for Four Asteroids." *Minor Planet Bul.* **35**, 167-171.

Weidenschilling, S.J., Chapman, C.R., Davis, D.R., Greenberg, R., Levy, D.H., Vail, S. (1987). "Photometric geodesy of main-belt asteroids. I - Lightcurves of 26 large, rapid rotators." *Icarus* **70**, 191-245.

Weidenschilling, S.J., Chapman, C.R., Davis, D.R., Greenberg, R., Levy, D.H. (1990). "Photometric geodesy of main-belt asteroids. III - Additional lightcurves." *Icarus* **86**, 402-447.

5426 SHARP: A PROBABLE HUNGARIA BINARY

Brian D. Warner
Center for Solar System Studies – Palmer Divide Station
446 Sycamore Ave.
Eaton, CO 80615 USA
brian@MinorPlanetObserver.com

Vladimir Benishek
Belgrade Astronomical Observatory
Belgrade, SERBIA

Andrea Ferrero
Bigmuskie Observatory
Mombercelli, Asti, ITALY

(Received: 9 April)

Initial CCD photometry observations of the Hungaria asteroid 5426 Sharp in 2014 December and 2015 January at the Center of Solar System Studies-Palmer Divide Station in Landers, CA, showed attenuations from the general lightcurve, indicating the possibility of the asteroid being a binary system. The secondary period was almost exactly an Earth day, prompting a collaboration to be formed with observers in Europe, which eventually allowed establishing two periods: P_1 = 4.5609 ± 0.0003 h, A_1 = 0.18 ± 0.01 mag and P_2 = 24.22 ± 0.02 h, A_2 = 0.08 ± 0.01 mag. No *mutual events, i.e.,* occultations and/or eclipses, were seen, therefore the asteroid is considered a *probable* and not *confirmed* binary.

Observations of the Hungaria asteroid 5426 Sharp were made by Warner at the Center for Solar System Studies-Palmer Divide Station (CS3-PDS) starting on 2014 December 29. These were follow-up to earlier work by Warner (2012) which found P = 4.56 h and A = 0.25 mag. The lightcurve was rated U = 2 on the asteroid lightcurve database rating system (LCDB; Warner *et al.*, 2009). Based on a high albedo derived from WISE observations (Masiero, 2011), Sharp is a member of the Hungaria *collisional family*, meaning it is a remnant of the parent body and probably of taxonomic type E.

The initial data from CS3-PDS showed attenuations from the general lightcurve that might be attributed to a satellite. A preliminary dual-period analysis by Warner using *MPO Canopus* found a secondary period of about 24 hours, making it nearly impossible to resolve the period with some certainty without observations from stations well removed in longitude.

OBS	Telescope	Camera
Warner	0.35-m *f*/9.1 Schmidt-Cass	STL-1001E
Benishek	0.35-m *f*/10 Schmidt-Cass	ST-8XME
Ferrero	0.30-m *f*/8.0 Ritchey-Chretien	ST-9

Table I. List of observers and equipment.

Obs	Dates (2014/2015)	Sessions
Warner (CS3-PDS)	12/29-01/02 14 19	1-5 8
Benishek (SAO)	01/15 16	6 7
Ferrero (BO)	01/24 26	10 11

Table II. Dates of observation for each observer. The Sessions column gives the session numbers shown in the lightcurve legend.

A collaboration was formed with Benishek (working at Sopot Astronomical Observatory) and Ferrero, which eventually allowed resolving the system parameters. Tables I and II list the observers, equipment used, and the dates that each person made observations. All exposures were unfiltered and ranged from 180 to 300 sec.

All three observers used *MPO Canopus* to measure the images. The Comp Star Selector utility found up to five solar-colored stars for each session. The magnitudes for the comparisons were taken from the MPOSC3 catalog, which is based on the 2MASS catalog converted to the BVRcIc system using formulae developed by Warner (2007). Benishek and Ferrero sent *MPO Canopus* export data sets to Warner for period analysis. This was also done in in *MPO Canopus,* which incorporates the FALC Fourier analysis algorithm developed by Harris (Harris *et al.,* 1989) and modified by Warner to allow subtracting a Fourier model lightcurve from a data set to search for a secondary period.

In the "No Sub" and "P1" lightcurves presented here, the "Reduced Magnitude" is Johnson V corrected to unity distance by applying $-5*\log(r\Delta)$ to the measured sky magnitudes with r and Δ being, respectively, the Sun-asteroid and Earth-asteroid distances in AU. The magnitudes in the "P2" are relative to the average magnitude of the "P1" lightcurve, or V = 15.15. The magnitudes were normalized to a phase angle of α = 19.5° using G = 0.43, which is the default for type E asteroids in the asteroid lightcurve database (LCDB; Warner *et al.*, 2009). The horizontal axis is the rotation phase, ranging from –0.05 to 1.05.

The "No Sub" lightcurve shows the entire data set when searching for a single period. The deviations from the average lightcurve exceed the general noise and so prompted the dual period search, which involves finding a single period, primary solution and subtracting that to find a secondary period. The resulting secondary period is subtracted to find a revised primary period. That is used to find a revised secondary period. The process continues until both periods stabilize.